

Critical behavior of iron borate of yttrium-iron garnet

A. L. Irshinskii, V. I. Ozhogin, V. M. Cherepanov, and S. S. Yakimov

I. V. Kurchatov Institute of Atomic Energy

(Submitted 8 September 1978)

Zh. Eksp. Teor. Fiz. 76, 1111-1122 (March 1979)

Mössbauer spectra are investigated and magnetization measurements are made on monocrystalline specimens of iron borate, FeBO_3 , and of yttrium-iron garnet, $\text{Y}_3\text{Fe}_5\text{O}_{12}$, near the Curie temperature in external magnetic fields from 0 to 30 kOe. The temperature and field dependences of the reduced magnetizations of the sublattices are obtained in both materials. The values of the critical exponents are determined in the temperature interval $7 \cdot 10^{-4} \leq (T - T_c)/T_c \leq 10^{-2}$: $\beta = 0.37 \pm 0.01$, $\delta = 3.9 \pm 0.02$, $\gamma = \gamma' = 1.2 \pm 0.1$ for FeBO_3 and $\beta = 0.39 \pm 0.01$, $\delta = 4.3 \pm 0.2$, $\gamma = \gamma' = 1.33 \pm 0.03$ for $\text{Y}_3\text{Fe}_5\text{O}_{12}$. The experimentally found dependence of the values of the critical exponents on the dimensionality of the order parameter is compared with the results of scaling-theory calculations.

PACS numbers: 75.40.Bw, 75.50.Dd, 76.80.+y

INTRODUCTION

The study of the critical behavior of magnetic materials near the magnetic ordering temperature T_c or T_N is of significant interest, since there has recently arisen a possibility of comparing the experimentally obtained values of the magnitudes of the critical exponents and critical amplitudes with predictions of scaling theory. The power laws that describe the principal thermodynamic characteristics of a system in the vicinity of T_c have the form

$$\begin{aligned} \bar{M}(t, 0) &= B(-t)^\beta, \quad \bar{M} = M(t, H)/M(-1, 0), \\ M(0, H) &= D(H)^{1/\delta}, \quad H = g\mu_B SH/kT_c, \end{aligned} \quad (1)$$

$$\bar{\chi}(t, 0) = \frac{\partial \bar{M}}{\partial H} \Big|_{H=0} = \begin{cases} \Gamma'(-t)^{-\gamma}, & t < 0 \\ \Gamma(t)^{-\gamma}, & t > 0 \end{cases}, \quad t = \frac{T - T_c}{T_c},$$

where T_c is the Curie temperature, \bar{H} is the reduced external magnetic field, $\bar{M}(t, \bar{H})$ is the reduced magnetization (the order parameter), t is the reduced temperature, and $\bar{\chi}$ is the reduced susceptibility; β , δ , γ , and γ' are the critical exponents, and B , D , Γ , and Γ' are the critical amplitudes.

According to the universality principle,¹ the critical behavior of magnetic materials depends chiefly on the dimensionality d of the lattice and on the number of the order-parameter components n , which in real crystals is determined by the relative value and type of magnetic anisotropy.

This paper reports the results of an investigation of the distinctive features of the critical behavior of two-sublattice crystals with a dominant antiferromagnetic exchange interaction: weakly ferromagnetic iron borate and ferrimagnetic yttrium-iron garnet (YIG), which have different types of magnetic anisotropy.

The data at present available on study of the behavior of magnetic materials near T_c have been obtained principally by magnetic measurement methods. These methods are comparatively simple and universal, but they have a number of disadvantages. The most important among these is the impossibility of making the measurements in the absence of an external field, so that extrapolation must be used to determine T_c and

the spontaneous magnetization. Therefore the data of different authors, even when obtained in studies of identical materials, often differ greatly from each other. In particular, for YIG the published values of the critical exponent β cover such a wide interval²⁻⁷—from 0.313 to 0.75—that this practically eliminates the possibility of verifying theoretical predictions.

In contrast to magnetic measurements, Mössbauer spectroscopy makes it possible to measure the values of the magnetizations of the individual sublattices and of their spatial orientations both in an external field and when $H = 0$. On the other hand, it seemed important to carry out both Mössbauer and magnetic measurements on the same specimens, in order to compare the potentialities of the two methods. And finally, an important factor in the choice of materials for investigation was the fact that for FeBO_3 and YIG the proportionality of the hyperfine fields on the ^{57}Fe nuclei to the sublattice magnetizations had been confirmed by comparison of the data from neutron-diffraction, Mössbauer, and NMR measurements over a wide temperature range all the way to $0.95 T_c$.⁸⁻¹¹

EXPERIMENT

The FeBO_3 monocrystals were plates of almost exact hexagonal shape, with dimensions $1 \times 1 \times 0.05$ mm. The plane of the plates coincided with the basal plane (111). For the Mössbauer measurements, a mosaic specimen was prepared from these plates, with total area ≈ 1 cm^2 ; this specimen ensured observation of a sufficiently marked effect of resonance absorption with the natural content of isotope ^{57}Fe . The FeBO_3 specimen for magnetic measurements was a disk of diameter 4 mm and height 3 mm, cemented together from plates of the same batch in such a way that the planes of the individual plates coincided as nearly as was possible.

The YIG specimens used were monocrystalline plates of thickness 120 μm , cut in the (110) plane. The diameter of the specimen for the Mössbauer measurements was 1 cm; of the specimen for the magnetic measurements, 4 mm.

The specimens were placed in a high-temperature, low-gradient furnace, which for measurements in an

external field was mounted between the poles of an electromagnet in such a way that the field could be applied in the plane of the specimens. The direction \mathbf{k}_γ of the beam of γ quanta was perpendicular to \mathbf{H} . The Mössbauer measurements were made with a one-channel analyzer under conditions of constant velocity of motion of the source (^{57}Co in a chromium matrix, of activity ≈ 100 mCi), and also with a many-channel analyzer "NOKIA" LP-4840. The spectrometers were calibrated against the known spectra of hematite and of sodium nitroprusside; the instrumental linewidth was 0.3 to 0.5 mm/sec. The Mössbauer spectra were processed on a computer by the method of least squares, on the assumption of a Lorentz line shape, with the program described in Ref. 12.

For the magnetic measurements, a vibration magnetometer, model PAR-155, was used; it was also used to determine the direction of easy magnetization [111] in the (110) plane of the YIG specimens. This made it possible to orient them in such a way that the external field was parallel to the [111] axis with accuracy $\sim 3^\circ$. As will be shown below, such orientation appreciably simplifies the deciphering of the YIG spectra.

The temperature of the specimens, both in the magnetic and in the Mössbauer method, was measured by the same copper-constantan thermocouple and was kept constant by an automatic thermoregulator, with accuracy no worse than $5 \cdot 10^{-2}$ K over a period of 8 to 10 hours. The relative drop of the temperature along the specimen did not exceed 10^{-4} . The Curie points of FeBO_3 and of YIG were determined by the method of temperature scanning in the Mössbauer spectroscopy and were 348.6 ± 0.1 and 550.25 ± 0.05 K, respectively.

RESULTS AND DISCUSSION

1. FeBO_3 . Iron borate is one of the simplest among the rhombohedral antiferromagnets with weak ferromagnetism (AWF), since the Fe^{3+} ions, located at crystallographically equivalent positions, are in the S state. The crystal symmetry (space group D_{3d}^6) allows the existence of a weak-ferromagnetism vector $\mathbf{m} = (\mathbf{M}_1 + \mathbf{M}_2)/2M_0$ in the basal (111) plane, perpendicular to the third-order axis C_3 . Investigations of the magnetic properties⁹ and neutron-diffraction measurements¹⁰ have shown that the vectors \mathbf{m} and $\mathbf{l} = (\mathbf{M}_1 - \mathbf{M}_2)/2M_0$, and therefore also the sublattice magnetizations \mathbf{M}_1 and \mathbf{M}_2 , lie in the basal plane. According to the data of Ref. 13, at room temperature the effective field of uniaxial anisotropy, which keeps \mathbf{l} in the easy plane (111), is $H_A^u \approx 3$ kOe, whereas in the plane itself the anisotropy is vanishingly small ($H_A^l \leq 1$ Oe).

The effect of the inducing of magnetic ordering by an external field in FeBO_3 near T_c has already been studied¹⁴ by the method of Mössbauer spectroscopy. But the analysis of the data in the cited paper was limited to the framework of the phenomenological theory of this effect presented in Ref. 15. Below, we communicate the results of a more detailed investigation of the induction effect in FeBO_3 , for the purpose of determining the critical magnetic parameters of this material.

Characteristic Mössbauer spectra of iron borate in the vicinity of T_c are shown in Fig. 1. We note that although our specimen consisted of a large number of fine crystals, because of the almost complete absence of anisotropy in the basal plane, 100 Oe of external field was entirely sufficient to make the specimen a single domain. The directions of the vectors \mathbf{m} in the individual monocrystals coincide with each other and with \mathbf{H} , while \mathbf{l} is directed perpendicular to \mathbf{H} , as is corroborated by the relation between the intensities of the two adjacent outer lines ($I_1 : I_2 \approx 3 : 1.2$; see spectrum 1). In the paramagnetic temperature range, a weakly resolved quadrupole doublet was observed; its asymmetry is due to the fact that the principal axis of the axial tensor of the electric field gradient (EFG) at the ^{57}Fe nuclei, which coincides in direction with C_3 , makes an angle of 45° with \mathbf{k}_γ (spectrum 2). The value of the quadrupole splitting, $\Delta E_Q = 0.37 \pm 0.01$ mm/sec, was found to be, for most of the measured spectra, much smaller than the Zeeman splitting ΔE_H of the nuclear levels; therefore the values of the effective fields H_{eff} at the nuclei could be calculated by the well-known expression for the eigenvalues of the Hamiltonian of combined magnetic and electric hyperfine (hf) interaction in the case of an EFG tensor with its symmetry axis directed at angle θ to the magnetic axis¹⁶ (in FeBO_3 , $\theta = \pi/2$):

$$E = -g\mu_n H m_l + (-1)^{|m_l|+1/2} \frac{eQV_{zz}}{4} \frac{3 \cos^2 \theta - 1}{2}. \quad (2)$$

In the calculation of H_{eff} from spectra for which ΔE_Q becomes comparable with ΔE_H , we included corrections to (2) for the additional shift of the sublevels of the excited state of the nucleus ($I = 3/2$); the procedure for introducing them is described below, in the discussion of the spectra of YIG.

Application of an external field $H \approx 30$ kOe at $T \approx T_c$ causes induction of an effective field $H_{\text{eff}} \approx 100$ kOe at

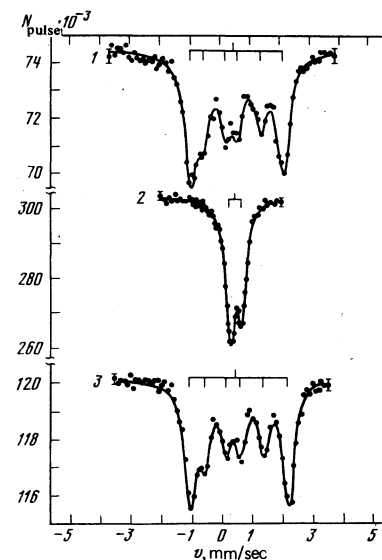


FIG. 1. Mössbauer spectra of FeBO_3 near T_c (the axis C_3 makes an angle 45° with the direction of \mathbf{k}_γ ; $\mathbf{H} \parallel (111)$: 1) $H = 0.1$ kOe, $T - T_c = -1.4$ K; 2) $H = 0$, $T = T_c$; 3) $H = 29.6$ kOe, $T = T_c$.

the nuclei; this indicates the restoration of magnetic order in the specimen, with $|l| \approx 0.2$. The intensity ratio $I_1 : I_2 \approx 3 : 1.3$, with allowance for the superposition of fields $H_{\text{eff}} = H_{\text{hf}} + H$, directly indicates the restoration of a two-sublattice AWF structure with $l \perp H$ (see spectrum 3 in Fig. 1). By a simple construction, similar to that used in Ref. 17, one can show that

$$H_{\text{eff}}^2 \approx H_{\text{hf}}^2 + H^2 + HH_{\text{hf}}(H + H_D)/H_E. \quad (3)$$

Under our conditions $H_E \gg H_{\text{hf}}$; therefore

$$H_{\text{hf}} \approx (H_{\text{eff}}^2 - H^2)^{1/2}. \quad (4)$$

Figure 2 shows the results of a measurement of the variation of the reduced hyperfine field, which is proportional to the magnetization of the sublattices:

$$\tilde{H}_{\text{hf}}(T, H) = H_{\text{hf}}(T, H)/H_{\text{hf}}(0, 0) = M(T, H)/M(0, 0) = \sigma(T, H), \quad (5)$$

where $M = |M_1| = |M_2|$. The critical exponents and amplitudes found from the $H_{\text{hf}}(T, H)$ data by formulas (1) for FeBO_3 are given in Tables I and II.

The values of $\tilde{\chi}(t, 0)$ were determined by numerical differentiation of the magnetization isotherms at $H \rightarrow 0$ with allowance for the magnetic measurement data. The calculation of the values of the critical parameters was carried out by the method of least squares; only the values of the critical exponents and amplitudes were varied, while T_c was held fixed. In addition, an analysis was made of the dependence of β on the upper bound t_m of the temperature interval. It was established that the value of β stabilizes near the value $\beta = 0.37 \pm 0.01$ when $t_m \leq 10^{-2}$; that is, over the temperature interval $7 \cdot 10^{-4} \leq |t| \leq 10^{-2}$. A similar variation $\beta(t_m)$ has also been detected in many other materials.¹⁸ This apparently also explains some divergence of our value of β from the value $\beta = 0.354 \pm 0.005$ found earlier¹⁹ by the Mössbauer-spectroscopy method on a monocrystal of FeBO_3 , but determined over a wider interval than ours, $4 \cdot 10^{-4} \leq |t| \leq 6 \cdot 10^{-2}$. In Ref. 20 the value $\beta = 0.338 \pm 0.005$ was obtained by the NMR method in the interval $10^{-2} \leq |t| \leq 10^{-1}$, which extends still farther beyond the limits of the critical region. We note that in the calculation of the critical exponents, the authors of Refs. 19 and 20 used the values of T_c themselves as variable parameters, whereas in our measurements the temperature T_c was determined independently. On the

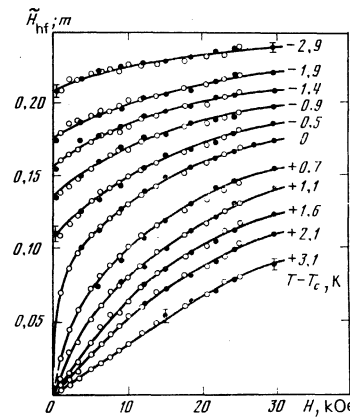


FIG. 2. Magnetization isotherms of FeBO_3 : ● Mössbauer measurements, ○ magnetic measurements.

other hand, it was found that if one processes our data on the relation $H_{\text{hf}}(U, 0)$ over the wider interval $10^{-3} \leq |t| \leq 10^{-1}$, one gets the value $\beta = 0.353 \pm 0.012$,¹⁴ which agrees with the results of Ref. 19.

Figure 2 shows also the results of static magnetic measurements of the weakly ferromagnetic component $m_{\text{WF}}(T, H)$ in FeBO_3 , obtained with allowance for the $H_{\text{hf}}(T, H)$ data as follows.

In distinction from magnetic measurements on ordinary (exchange) ferromagnets, additional complications arise in magnetic measurements on AWF. The point is that besides the singular component $m_{\text{WF}}(T, H) = m_{\text{WF}}(T, 0) + \chi_{\text{WF}}(T)H$, due to the effect of induction, the expression for the magnetization contains also a regular component $m_{\text{AF}}(T, H) = \chi_{\text{AF}}(T)H$, caused by the purely antiferromagnetic susceptibility of the spin system. Separation of $m_{\text{WF}}(T, H)$ from the total signal

$$m(T, H) = m_{\text{WF}}(T, 0) + \chi_{\text{WF}}(T)H + \chi_{\text{AF}}(T)H \quad (6)$$

is a quite complicated independent problem. The errors in the determination of each contribution to (6), in themselves small, may distort the information about the critical behavior of $m_{\text{WF}}(T, H)$.

Therefore in order to separate $m_{\text{AF}}(T, H)$ from (6), we used instead of $m_{\text{WF}}(T, 0)$ the data on $H_{\text{hf}}(T, 0)$; $\chi_{\text{AF}}(T)$ was so chosen that $m_{\text{WF}}(T, H)$ agreed with $H_{\text{hf}}(T, H)$, as is shown in Fig. 2. The values of $\chi_{\text{AF}}^{-1}(T)$

TABLE I. Critical exponents.

Material	β	δ	ν	ν'	Method of determination*
FeBO_3	0.37 ± 0.01	3.9 ± 0.2	1.2 ± 0.1	1.2 ± 0.1	MS, M[DP]
	0.35 ± 0.007	3.9 ± 0.4	1.38 ± 0.08	1.0 ± 0.1	M ¹²
	0.338 ± 0.005	—	—	1.33 ± 0.03	NMR ²⁰
$\text{Y}_2\text{Fe}_2\text{O}_{11}$	0.39 ± 0.01	4.3 ± 0.2	1.33 ± 0.03	—	MS[DP]
	0.38 ± 0.005	4.42 ± 0.09	1.31 ± 0.01	—	M ²
	0.37 ± 0.05	4.65 ± 0.1	1.35 ± 0.01	—	MO ⁴
	0.35 ± 0.02	4.6 ± 0.2	1.32 ± 0.04	—	M ²
YFeO_3	0.36 ± 0.01	4.0 ± 0.4	1.0 ± 0.2	1.0 ± 0.2	MS ²³
Scaling theory, ϵ expansion					
$n=1$	0.34	4.462	1.24	—	} 30
$n=2$	0.36	4.460	1.30	—	
$n=3$	0.38	4.458	1.34	—	

*M, magnetic measurements; MS, Mössbauer spectroscopy; MO, magneto-optical measurements; [DP], data of this paper.

TABLE II. Critical amplitudes.

Material	B	D	Γ	$R_x = \Gamma D^{-5} B^{8-1}$
FeBO ₃	1.23±0.05	2.4±0.3	0.014±0.005	0.8±0.4
Y ₃ Fe ₅ O ₁₂	1.29±0.04	0.64±0.07	0.066±0.005	1.0±0.3

thus obtained are shown in Fig. 3, together with the values of the inverse total susceptibility $\chi_{\text{total}}^{-1}(T) = [\chi_{\text{WF}}(T) + \chi_{\text{AF}}(T)]^{-1}$. Since the values of $\chi_{\text{WF}}(T)$ were measured by the Mössbauer-spectroscopy method only in the interval $|T - T_c| \leq 3$ K, beyond its boundaries the $\chi_{\text{WF}}(T)$ relation was extrapolated according to the same power law as in the critical region.

One is struck by the significantly nonlinear variation of $\chi_{\text{AF}}^{-1}(T)$ in the neighborhood of T_c . A similar but less pronounced temperature variation of the perpendicular susceptibility in the neighborhood of T_N was observed by Bazhan in an AWF isomorph to iron borate, NiCO₃.²¹ In this connection, we also present in Table I the values of the critical exponents of FeBO₃ found by Wilson and Broersma²² on a polycrystalline specimen with a vibration magnetometer. It is seen that they differ markedly from the values that we obtained by the Mössbauer-spectroscopy method, with the exception of the exponent δ . This discrepancy can be explained on the following grounds. First, in Ref. 22 the values of T_c and $m(T, 0)$ were determined by the method of extrapolation to $H = 0$; and second, for subtraction of the contribution $m_{\text{AF}}(T)$ from $m(T, H)$, interpolation of the $\chi_{\text{AF}}(T)$ relation between room temperature and $T = 373$ K was used, which in the light of the anomaly that we have found in $\chi_{\text{AF}}(T)$ seems not altogether correct (the dotted line in Fig. 3).

From Fig. 3 it is also seen that the interpolated curve $\chi_{\text{AF}}^{-1}(T)$ intersects our curve $\chi_{\text{AF}}^{-1}(T)$ only near T_c , thanks to which the indices δ agree, but away from T_c these relations differ greatly.

Wilson and Broersma also treated the fulfillment of the predictions of scaling theory for FeBO₃ within the framework of the parametric form of the equation of state, and found three different sets of values of the

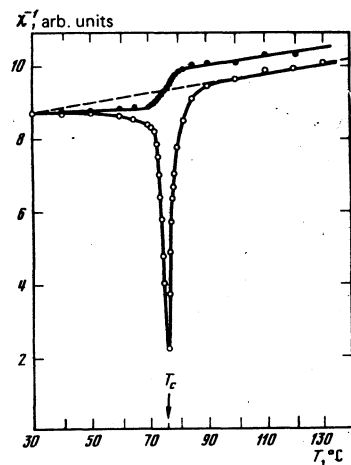


FIG. 3. Variation of inverse magnetic susceptibility of FeBO₃ with temperature: \circ $\chi_{\text{total}}^{-1}(T)$; \bullet $\chi_{\text{AF}}^{-1}(T)$. Dotted line: interpolation of χ_{AF}^{-1} according to the data of Ref. 22.

phenomenological parameters a and k of the theory for the regions below, near, and above T_c ; that is, there is no unique equation of state for the whole critical region. From analysis of our data for $H_{\text{hf}}(T, H) \approx l(T, H)$ it is evident that they not only satisfy one of the basic relations of scaling theory, $\gamma' = \beta(\delta - 1)$, but in contrast to Ref. 22 give $\gamma = \gamma'$. The equation of state in the critical temperature range is written in the form

$$M(t, H)/|t|^{\delta} = f(H/|t|^{\beta}). \quad (7)$$

The graph of the "scaling function" f obtained experimentally from the $H_{\text{hf}}(T, H)$ data, and shown in Fig. 4 on a logarithmic scale, shows that the magnetization isotherms break up into two branches, corresponding to $T < T_c$ and to $T > T_c$, and joining at $T \rightarrow T_c$. This indicates the presence of a single equation of state of FeBO₃ over the whole critical region $7 \cdot 10^{-4} \leq |t| \leq 10^{-2}$, satisfying the prediction of scaling theory. Unfortunately it is difficult to make a more detailed comparison of our data and of the results of Ref. 22, since in the latter no concrete data on $m(T, H)$ are given.

2. Y₃Fe₅O₁₂. In the YIG crystal, whose elementary cell is cubic (space group O_h^{10}), the Fe³⁺ ions are located at crystallographically nonequivalent sites, d with tetrahedral and a with octahedral environments. The [111] axes are the axes of easy magnetization, and the effective field of the cubic anisotropy is $H_A \approx 40$ Oe at room temperature.²³ The directions of the principal axes of the axially symmetric EFG tensor on the d sites coincide with [100] axes (three different directions), and on the a sites with [111] axes (four different directions).

In Fig. 5, curve 1 shows the Mössbauer spectrum of YIG at $T = T_c - 5.2$ K, taken in the weak external magnetic field that was necessary to make the specimen a single domain. The magnetization M lies in the plane of the plate, the (110) plane; $M \parallel H_{\text{hf}} \parallel [111]$. In this case, for all the iron ions in the d sublattice the angle $\theta = 54^\circ 44'$, and the value of the measurable quadrupole splitting is $\Delta E_{Qm}^d = 0$, whereas in the a sublattice the angle θ takes two values: $70^\circ 32'$ ($\Delta E_{Qm}^a = \Delta E_Q^a/3$) and 0° ($\Delta E_{Qm}^a = \Delta E_Q^a$). The Mössbauer spectrum of YIG is a superposition of three Zeeman sextets of lines with in-

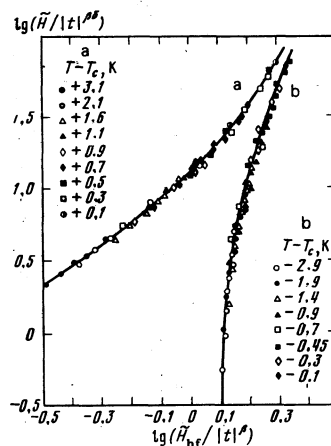


FIG. 4. Graph of the "scaling function" of FeBO₃ according to Mössbauer-measurement data: a, for $T > T_c$; b, for $T < T_c$.

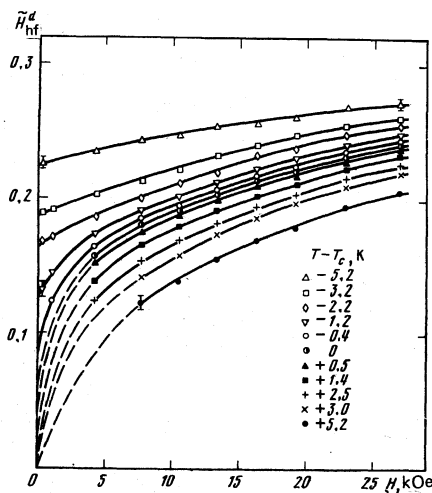


FIG. 8. Isotherms of the d sublattice magnetization of YIG.

and J_{ad}) value of the constant J_{ad} , and this apparently leads also to the proportionality of σ_a and σ_d in accordance with the universality principal.

The values of the critical exponents and amplitudes of YIG obtained according to formulas (1), in the reduced-field interval $2.5 \cdot 10^{-4} < \tilde{H} < 2 \cdot 10^{-2}$ and the reduced temperature interval $8 \cdot 10^{-4} \leq |t| \leq 10^{-2}$, are given in Table I and Table II. The upper limit of the temperature interval was determined as the temperature at which the variable value of the index β becomes stabilized for fixed T_c .

As in the case of FeBO_3 , analysis of the data on $\sigma(T, H) = 3\tilde{H}_{\text{eff}}^d(T, H) - 2\tilde{H}_{\text{eff}}^a(T, H)$ and of the values of the critical indices shows that they satisfy the basic scaling-theory relations $\gamma' = \beta(\delta - 1)$ and $\gamma = \gamma'$. The graph of the "scaling function" of the YIG breaks into two branches with $T < T_c$ and $T > T_c$, converging for $T \rightarrow T_c$; this also satisfies the prediction of scaling theory.

In Refs. 3 and 6 values of the critical exponents of YIG were obtained by the method of magnetic measurements; they are close to our results, within the limits of error, but differ from the results obtained in Refs. 2, 4, and 7. Berkner and Litster⁴ made magneto-optical measurements of $M(T, H)$ over the wide temperature interval $-2 \cdot 10^{-2} \geq t \geq -0.7$, which extends beyond the limits of the critical region; this can apparently explain the difference of their results from ours. In Refs. 2 and 7, extrapolations of $M(T, H)$ to zero field were used in the determination of T_c and $M(T, 0)$. The inaccuracy in the determination of T_c and $M(T, 0)$ in this case may be responsible for the difference of the values of critical exponents obtained in Refs. 2 and 7 from ours.

3. In both the crystals investigated, the magnetic elementary cell coincides with the crystallographic. According to Ref. 27, in this case the dimensionality of the order parameter $n \leq 3$. FeBO_3 is an AWF with anisotropy of the "easy plane" type and with a quite large value of the ratio $H_A^u/H_F \approx 10^{-3}$, whereas $\text{Y}_3\text{Fe}_5\text{O}_{12}$ is a two-sublattice ferrimagnet with small cubic an-

isotropy: $H_A^{1111}/H_F \approx 10^{-7}$. It may therefore be expected that the critical behavior of FeBO_3 will be close to that of the XY model ($n=2$), while the critical behavior of the YIG will be close to that of the Heisenberg model ($n=3$).

It is seen from Table I that the values of β , δ , and γ for YIG are in good agreement with the values of the critical exponents calculated to the second order by the $\varepsilon = 4 - d$ expansion method in scaling theory. Furthermore, the universal constant $R_x = \Gamma D^{-6} B^{6-1} = 1.0 \pm 0.4$ obtained from the experimental values of the critical amplitudes for YIG is close to the theoretical value 1.33 for $n=3$.

As regards the values of the critical exponents for FeBO_3 , β and γ agree, within the limits of experimental error, with the theoretical values, but the value of δ is significantly lower than that predicted for $n=2$. Table I shows, for comparison, the critical exponents, measured by the Mössbauer spectroscopy method,²⁸ of yttrium orthoferrite YFeO_3 , which according to the type of magnetic anisotropy may also be assigned to the class of easy-plane AWF.²⁹ They are close to the critical indices of FeBO_3 ; β agrees with the theoretical value for $n=2$, but δ and γ again deviate toward the values predicted by mean-field theory.

For our discussion, however, it is more important to explain not simply the agreement of experimentally obtained critical exponents with theoretical, since the latter have been calculated only in a certain approximation and are not final, but to compare their dependence on n with the dependence predicted within the framework of renormalization-group theory, which is maintained in all orders of the ε expansion that have been studied, above the first.³⁰

From a comparison of the values of the critical exponents of YIG and of iron borate (and also of yttrium orthoferrite) it follows that the best agreement with calculations on going from $n=3$ to $n=2$ is attained for the exponent β . For γ , the change does agree in sign, but it significantly exceeds the calculated; and the change of the index δ does not agree either in sign or in value with the theoretical. But when one takes into account the insufficient accuracy of determination of the exponents γ and β for AWF achieved in our experiment, it is difficult to draw a sure conclusion about the reason for such an anomaly in their critical behavior. For this purpose it is necessary not only to improve the accuracy of the measurements, but also to carry out investigations on other crystals, belonging to different universality classes.

We express our deep appreciation to K. K. Kikoin for his attention to this research, and we thank I. G. Aვაeva and Yu. M. Yakovlev for providing the FeBO_3 and $\text{Y}_3\text{Fe}_5\text{O}_{12}$ monocrystals.

¹L. P. Kadanoff, in: *Kvantovaya teoriya polya i fizika fazovykh perekhodov* (Quantum Field Theory and the Physics of Phase Transitions), Mir, 1975, p. 7.

²K. Ohbayashi and S. Iida, *J. Phys. Soc. Jpn.* **25**, 1187 (1968).

³K. Miyatani and K. Yoshikawa, *J. Appl. Phys.* **41**, 1272 (1970).

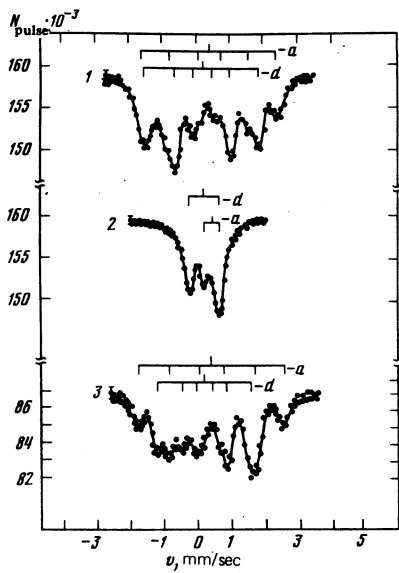


FIG. 5. Mössbauer spectra of $Y_3Fe_5O_{12}$ near T_c ($\mathbf{k}_\gamma \perp (110)$, $\mathbf{H} \parallel [111]$): 1) $H=0.3$ kOe, $T-T_c = -5.2$ K; 2) $H=0$, $T=T_c$; 3) $H=20$ kOe, $T=T_c$.

tensity ratio 6:3:1. But it is impossible to resolve the individual sextets from the iron ions in the a sublattice because of the small value of $\Delta E_Q^a = 0.50$ mm/sec. Processing of the spectrum by the method of least squares showed that it is a superposition of two sextets with intensity ratio $I_a : I_d \approx 2 : 3$ and $\Delta E_Q^a \approx 0$.

For the d sublattice of YIG in the temperature range $T_c - T \lesssim 10$ K, the energy of magnetic dipole interaction for the excited state of the ^{57}Fe nucleus becomes comparable with the energy of electric quadrupole interaction. Matthias, Schneider, and Steffen²⁴ made detailed numerical calculations of the energy of splitting of the magnetic sublevels of the nucleus with spin $I=3/2$ as a function of the angle θ and of the variable

$$y = 2\Delta E_{HF} / \Delta E_Q.$$

According to Ref. 24, for $0 < y \lesssim 10$ and $\theta \neq 0$ the value of the complete splitting ΔE of the spectrum (the distance between the first and sixth lines of a sextet) varies nonlinearly with H_{HF} , and this variation must be taken into account in order to obtain the correct value of H_{HF} . Thus for spectrum 1 in Fig. 5, $y=4.1$ and $H_{eff}/H_{HF} = 1.2$, where H_{eff} is the effective field on the ^{57}Fe nucleus without allowance for the variation of ΔE with y .

In Fig. 5, spectrum 3 represents the spectrum of YIG at $T=T_c$ and $H=20$ kOe. The specimen was so oriented that the direction of H coincided with one of the two $[111]$ directions in the (110) plane of the plate, and the processing of the spectra could be carried out just as in the preceding case. The numbers of Fe^{3+} ions in a and d sites, per elementary cell, are 16 and 24 respectively, and $M_d/M_a = 3/2$. Therefore the magnetization M_d is parallel and M_a antiparallel to M and H . Since the direction of H_{HF} is opposite to the direction of the magnetization of the corresponding sublattice,

$$H_m^a = H_{eff}^a + H, \quad H_m^d = H_{eff}^d - H,$$

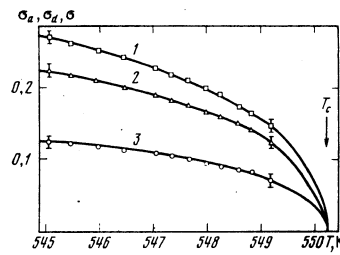


FIG. 6. Variation of the reduced magnetization of YIG with temperature in the absence of an external field: 1) $\sigma_a(T)$, 2) $\sigma_d(T)$, 3) $\sigma(T) = 3\sigma_d(T) - 2\sigma_a(T)$.

where H_m is the directly measurable field on the nucleus according to the spectrum. From H_{eff}^a and H_{eff}^d , the values of H_{HF}^a and H_{HF}^d were found by use of the results of Ref. 24.

The behavior of the reduced sublattice magnetizations

$$\sigma_a = H_{HF}^a(T, 0) / H_{HF}^a(0, 0), \quad \sigma_d = H_{HF}^d(T, 0) / H_{HF}^d(0, 0),$$

and also of the resultant reduced magnetization $\sigma = 3\sigma_d - 2\sigma_a$, in the absence of a magnetic field in the temperature interval 545–550 K, is shown in Fig. 6. Figures 7 and 8 give magnetization isotherms $\sigma_a = \tilde{H}_{HF}^a(T, H)$ and $\sigma_d = \tilde{H}_{HF}^d(T, H)$ for the a and d sublattices.

Over the interval $T = T_c \pm 5$ K, the value of σ_a was found to be proportional to σ_d both in an external magnetic field and in its absence, with $\sigma_a/\sigma_d = 1.20$. As was shown in Refs. 25 and 26, the ratio σ_a/σ_d changes from 1.17 to 1.23 when the temperature changes from 4.2 to 360 K. The exchange constants found for YIG in these references have the following values:

$$J_{ad} = 22.5 \text{ cm}^{-1}, \quad J_{dd} = 2.0 \text{ cm}^{-1}, \quad J_{aa} = 0.5 \text{ cm}^{-1}.$$

Near T_c , the critical behavior of YIG is determined principally by the much larger (as compared with J_{aa}

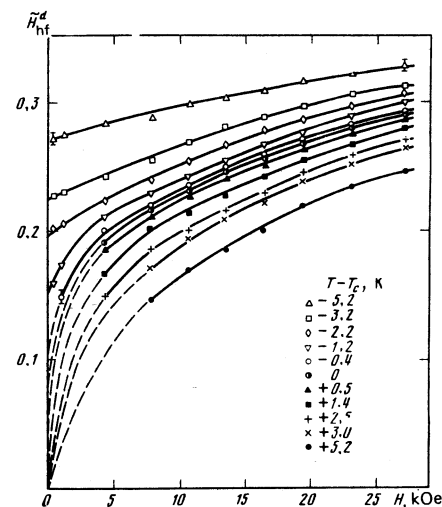


FIG. 7. Isotherms of the a sublattice magnetization of YIG.

- ⁴D. D. Berkner and J. D. Litster, AIP Conf. Proc. **10**, Part 2, 894 (1972).
- ⁵A. I. Okorokov and Ya. A. Kasman, Fiz. Tverd. Tela **14**, 3065 (1972) [Sov. Phys. Solid State **14**, 2622 (1973)].
- ⁶S. Araj, A. A. Stelmach, and E. E. Anderson, Int. J. Magn. **4**, 173 (1973).
- ⁷I. K. Kamilov, Kh. K. Aliev, and M. M. Magomedov, Pis'ma, Zh. Eksp. Teor. Fiz. **19**, 128 (1974) [JETP Lett. **19**, 78 (1974)].
- ⁸M. Pernet, D. Elmaleh, and J. Joubert, Solid State Commun. **8**, 1583 (1970).
- ⁹M. P. Petrov, G. A. Smolenskiĭ, A. P. Paugurt, S. A. Kizhaev, and M. K. Chistov, Fiz. Tverd. Tela **14**, 109 (1972) [Sov. Phys. Solid State **14**, 87 (1972)].
- ¹⁰E. Prince, J. Appl. Phys. **36**, 1845 (1965).
- ¹¹J. D. Litster and G. B. Benedek, J. Appl. Phys. **37**, 1320 (1966).
- ¹²V. I. Nikolaev, V. S. Rusakov, and S. S. Yakimov, Preprint IAE-2541, 1975.
- ¹³L. V. Velikov, A. S. Prokhorov, E. G. Rudashevskii, and V. N. Seleznev, Zh. Eksp. Teor. Fiz. **66**, 1847 (1974) [Sov. Phys. JETP **39**, 909 (1974)].
- ¹⁴S. S. Yakimov, V. I. Ozhogin, V. Ya. Gamlitskii, V. M. Cherepanov, and S. D. Pudkov, Phys. Lett. **39A**, 421 (1972).
- ¹⁵A. S. Borovik-Romanov and V. I. Ozhogin, Zh. Eksp. Teor. Fiz. **39**, 27 (1960) [Sov. Phys. JETP **12**, 18 (1961)].
- ¹⁶G. K. Wertheim, Mössbauer Effect: Principles and Applications, Academic Press, 1964 (Russ. transl., Mir, 1966).
- ¹⁷V. I. Ozhogin, IEEE Trans. Magn. MAG-12, 19 (1976).
- ¹⁸C. Hohenemser, Proc. Int. Conf. Mössbauer Spectroscopy, Cracow, **2**, 239 (1975).
- ¹⁹M. Eibschütz, L. Pfeiffer, and J. W. Nielsen, J. Appl. Phys. **41**, 1276 (1970).
- ²⁰V. D. Doroshev, N. M. Kovtun, V. N. Seleznev, V. M. Siryuk, and É. N. Ukraintsev, Fiz. Tverd. Tela **17**, 514 (1975) [Sov. Phys. Solid State **17**, 321 (1975)].
- ²¹A. N. Bazhan, Zh. Eksp. Teor. Fiz. **66**, 1086 (1974) [Sov. Phys. JETP **39**, 531 (1974)].
- ²²D. M. Wilson and S. Broersma, AIP Conf. Proc. **24**, 285 (1975); Phys. Rev. **B14**, 1977 (1976).
- ²³T. N. Belozerskiĭ, Yu. P. Khimich, and Yu. M. Yakovlev, Fiz. Tverd. Tela **14**, 1164 (1972) [Sov. Phys. Solid State **14**, 993 (1972)].
- ²⁴E. Matthias, W. Schneider, and R. M. Steffen, Ark. Fys. **24**, 97 (1963).
- ²⁵R. Gonano, E. Hunt, and H. Meyer, Phys. Rev. **156**, 521 (1967).
- ²⁶E. L. Boyd, V. L. Moruzzi, and J. S. Smart, J. Appl. Phys. **34**, 3049 (1963).
- ²⁷D. Mukamel and S. Krinsky, Phys. Rev. **B13**, 5056 (1976).
- ²⁸V. M. Cherepanov and S. S. Yakimov, Pis'ma Zh. Eksp. Teor. Fiz. **19**, 764 (1974) [JETP Lett. **19**, 392 (1974)].
- ²⁹V. I. Ozhogin, V. M. Cherepanov, and S. S. Yakimov, Zh. Eksp. Teor. Fiz. **67**, 1042 (1974) [Sov. Phys. JETP **40**, 517 (1974)].
- ³⁰K. G. Wilson and J. Kogut, The Renormalization Group and the ϵ Expansion, Phys. Reports **12C**, 75-200 (1974) (Russ. transl., Mir, 1975, p. 124).

Translated by W. F. Brown, Jr.

Simultaneous electronic transition $\text{Sm}^{2+}-\text{Sm}^{3+}$ and $\text{Yb}^{2+}-\text{Yb}^{3+}$ in $\text{Sm}_{1-x}\text{Yb}_x\text{S}$

G. A. Krutov, A. E. Sovestnov, and V. A. Shaburov

Leningrad Institute of Nuclear Physics, USSR Academy of Sciences

(Submitted 18 September 1978)

Zh. Eksp. Teor. Fiz. **76**, 1123-1127 (March 1979)

The method of the x-ray K-line shift [O. I. Sumbaev, Sov. Phys. Usp. **21**, 141 (1978)] is used to investigate the electron structure of Sm and Yb in $\text{Sm}_{1-x}\text{Yb}_x\text{S}$ ($0 \leq x \leq 1.77 \leq T \leq 1000$ K). A smooth increase of the valence of Sm with increase of x is observed, as well as a simultaneous change of the valence of Yb (at high temperature). It is shown that the observed effect is due to the departure of the 4f electrons of Sm and Yb into the conduction band. The valence change η_{Sm} is practically proportional to x and $\eta_{\text{Sm}} \approx 0.4$ at $x = 0.8$. The dependence of η_{Yb} on x correlates well with the concentration of the trivalent Sm ions in the sample, and reaches a value $\eta_{\text{Yb}} \approx 0.4$ at the maximum.

PACS numbers: 71.25.Tn, 32.30.Rj

1. INTRODUCTION

The mechanism of isomorphic phase transitions in solid solutions of SmS with monosulfides of trivalent rare-earth elements (REE) such as $\text{Sm}_{1-x}\text{R}_x\text{S}$ has been established quite reliably (see, e.g., the reviews¹). This transition is a particular case of the well known phenomenon of variable valence of the REE, and is due to the departure of the 4f electrons of Sm to the conduction band. It is assumed that the $\text{Sm}^{2+}-\text{Sm}^{3+}$ transition is initiated by the internal lattice ("chemical") pressure

produced in the SmS lattice upon penetration of small (compared with Sm) trivalent RE atoms $d_{\text{SmS}} = 5.97 \text{ \AA}$; $5.8 \geq d_{\text{R}^{3+}\text{S}} \geq 5.4 \text{ \AA}$). In the phase transition these trivalent atoms are passive: unlike Sm, which acquires a valence ≈ 2.6 in the transition, the valence of R^{3+} remains unchanged.²

Less investigated are the electronic properties of solid solutions of SmS based on monosulfides of divalent REE ($\text{Sm}_{1-x}\text{Eu}_x\text{S}$ and $\text{Sm}_{1-x}\text{Yb}_x\text{S}$).

The parameters of the EuS and YbS lattices are 5.97